

A11100 995776

NBS
PUBLICATIONS

NAT'L INST. OF STAND & TECH



A11106 419443

NBSIR 82-2524

Effects of Water and Other Dielectrics on Crack Growth

U.S. DEPARTMENT OF COMMERCE
National Bureau of Standards
Center for Materials Science
Fracture and Deformation Division
Washington, DC 20234

May 1982

Interim Report

Prepared for
Office of Naval Research
Department of the Navy
Arlington, VA

QC
100
.U56
82-2524
1982
c. 2

NBSIR 82-2524

JUL 7 1982

Not ac. - Circ.

QC100

.456

NO 82 2524

1982

C 2

**EFFECTS OF WATER AND OTHER
DIELECTRICS ON CRACK GROWTH**

S. M. Wiederhorn, S. W. Freiman, E. R. Fuller, Jr.
and C. J. Simmons

U.S. DEPARTMENT OF COMMERCE
National Bureau of Standards
Center for Materials Science
Fracture and Deformation Division
Washington, DC 20234

May 1982

Interim Report

Prepared for
Office of Naval Research
Department of the Navy
Arlington, VA



U.S. DEPARTMENT OF COMMERCE, Malcolm Baldrige, *Secretary*
NATIONAL BUREAU OF STANDARDS, Ernest Ambler, *Director*

Effects of Water and other Dielectrics on Crack Growth

S. M. Wiederhorn, S. W. Freiman, E. R. Fuller, Jr.
and C. J. Simmons

National Bureau of Standards
Washington, D.C. 20234

ABSTRACT

The effect of water and a variety of organic liquids on the crack growth rate in soda lime silica glass was investigated. When water is present in organic liquids, it is usually the principal agent that promotes subcritical crack growth in glass. In region I, subcritical crack growth is controlled primarily by the chemical potential of the water in the liquid; whereas in region II, crack growth is controlled by the concentration of water and the viscosity of the solution formed by the water and the organic liquid. In region III, where water does not affect crack growth, the slope of the crack growth curves can be correlated with the dielectric constant of the liquid. It is suggested that these latter results can be explained by electrostatic interactions between the environment and charges that form during the rupture of Si-O bonds.

Effects of Water and other Dielectric Fluids on Crack Growth

S. M. Wiederhorn, S. W. Freiman, E. R. Fuller, Jr.

and C. J. Simmons

National Bureau of Standards

Washington, D.C. 20234

1. Introduction:

Subcritical crack growth in glasses is believed to result primarily from a stress-enhanced chemical reaction between a chemical environment, usually water, and the Si-O bonds of the glass. The reaction occurs preferentially at crack tips where stresses are high. Prior investigations of subcritical crack growth in glass have indicated a rather complex dependence of crack velocity on the applied stress intensity factor and on the amount of water in the environment. If crack velocity is plotted as either an exponential, or power function of applied stress intensity factor, a trimodal curve is obtained, Figure 1; each of the three regions of the curve results from a different mechanism of crack growth.^{1,2}

Region I crack growth behavior is characterized by a dependence of crack velocity on stress intensity factor, K_I , and on the partial pressure of water in the environment.¹ If either of these two quantities are increased, the crack velocity is observed to increase. Crack growth studies conducted in either nitrogen gas¹ or in alcohols^{3,4} suggest that

the crack velocity is reaction rate limited in region I, and therefore, is controlled by the chemical potential of water in the environment at any level of applied stress intensity. Hence, identical crack growth behavior should be obtained in environments in which the chemical potential of water is the same.

Region II crack growth behavior is also characterized by a dependence of crack velocity on the amount of water in the environment. In contrast to region I behavior, however, the crack velocity in region II does not depend strongly on the applied stress intensity factor. Theoretical interpretations of region II crack growth behavior lead to the conclusion that the crack velocity is controlled by the rate of transport of water from the environment to the crack tip.^{1,2,5} Although it is recognized that crack growth in region II is limited by factors that affect transport processes, experimental data to quantify this relation have not yet been obtained.

Region III crack growth behavior is characterized by a strong dependence of crack growth rate on stress intensity factor, and by a complete absence of any dependence of crack growth rate on water in the environment. Of the three regions of crack growth, region III behavior is the least understood. Region III crack growth has been observed in vacuum for a variety of commercial silicate glasses, but not for glasses that have a high concentration (>90 percent) of silica.⁶ Because of these observations it has been suggested that region III crack growth is controlled by fracture mechanisms that do not depend on environment.

Studies of region III crack growth in normal alcohols, however, conflict with this view.^{3,4} In normal alcohols, it has been shown by Freiman³ that the slope of the crack growth curves is not as steep as that obtained in vacuum, or in dry nitrogen. Furthermore Freiman³ and Richter⁴ have demonstrated that the positions of the crack growth curves depend on the chain length of the alcohol. Hence, in some cases an environmental dependence of region III crack growth is apparent.

This paper provides additional experimental data to clarify our understanding of subcritical crack growth in glass. Crack growth data obtained in alcohols confirm the proposed role of chemical potential in controlling the crack growth rate in region I. In region II, however, water concentration, rather than chemical potential, will be shown to control the rate of crack growth. A model for diffusion controlled crack growth is developed to show that fluid viscosity is also a parameter of importance. Finally, data is presented to confirm the fact that crack growth behavior in region III is affected by the chemical composition of the test media. Crack growth in region III is influenced by an electrostatic interaction between the environment and charges that develop at the crack tip during the fracture process.

2. Experimental Procedure

Crack propagation studies were conducted on soda lime silica glass in normal alcohols, heptane, formamide, trichloroethylene and acetonitrile. The alcohols were selected as test media because the

solubility of water in alcohols decreases with increasing alcohol chain length, so that it is possible to produce solutions of water and alcohol that have equal chemical potentials even though they contain different concentrations of water. These solutions were used to elucidate the effect of water concentration on region II crack growth behavior. Where possible, the partial pressure of water in the solutions was determined by direct analysis with an immersible hygrometer. The amount of water in solution, (i.e. the concentration) was determined by the Karl-Fisher technique. This procedure permitted us to make independent comparisons of effects of chemical composition and chemical potential on crack growth in region II. A set of ethyl and butyl alcohol solutions, used primarily for the study of region I crack growth, was made by adding predetermined amounts of water to the "pure" alcohols. The chemical potential of these solutions were then determined by reference to phase equilibrium diagrams for these solutions.^{7,8} The viscosities of solutions used for region II crack growth studies were determined by direct analysis using a Cannon-Fenske viscosimeter (Table 1).

Crack growth studies in region I, II and III were conducted on soda-lime-silica glass microscope slides using both the double cantilever beam technique and the double torsion technique.^{9,10} Region I studies were conducted using double cantilever beam specimens, 7 x 25 x 2 mm, with a 0.5 mm deep groove along the midplane on both sides of the specimen to control the direction of crack growth. Double torsion specimens, (ungrooved) 75 x 25 x 1 mm, were used for crack growth measurements in regions I, II and III. In regions I and II the load relaxation method

was used to collect crack growth data, whereas in region III, both load relaxation and constant displacement techniques were used.

Studies in region II were made in saturated alcohols prepared by mixing excess water with the alcohols and agitating the liquids several times a week for six months. A chemical analysis of the water in solution and a measurement of the partial pressure of the water in the alcohol are presented in Table 1. With the exception of the octyl alcohol, all of the alcohols were found to be saturated with water. We were somewhat surprised by the observation that the octyl alcohol used in our study was not fully saturated, and have no explanation for this result. However, crack growth studies (region II) to be discussed below are consistent with this observation.

The double torsion technique was also used to investigate crack growth behavior in region III. To determine if the position of the crack velocity curve in alcohol differed significantly from that in dry nitrogen, crack propagation data were obtained by the relaxation method on the same specimen, first in dry nitrogen, then in alcohol. Three crack velocity curves were first obtained in nitrogen gas. Without disturbing the specimen, either methyl, amyl, or decyl alcohol were added to the test chamber and three more crack velocity curves were obtained. This procedure enabled us to reduce systematic variations and thus obtain crack propagation curves that accurately reflect the positions of the crack growth curves in alcohol, relative to those in dry nitrogen gas.

In a second study of region III crack growth, the constant displacement rate technique was used to obtain crack growth data in dry nitrogen gas, methyl alcohol, decyl alcohol, acetonitrile and heptane. At least 10 experimental runs were made at each displacement rate in order to reduce systematic error that resulted in variations in measured K_I . The mean value and standard deviation of K_I were obtained for each displacement rate measurement, and at least three displacement rates were used to determine the position and slope of each crack velocity curve. Displacement rates used in these studies were selected so that the velocities were in region III. The velocities had to be low enough, however, to assure that cavitation of the fluid at the crack tip did not occur.¹¹ Some experimental results in region III were also obtained on vitreous silica (C7940) in octyl alcohol using the applied moment, double cantilever beam technique.¹² Since silica glass normally does not exhibit subcritical crack growth in region III,⁶ the demonstration of subcritical crack growth in octyl alcohol is a clear indication of an interaction between glass and alcohol.

3. Results

The crack propagation data for soda-lime-silica glass in ethyl and butyl alcohols are shown in Figures 2,3. The shapes and positions of these curves are similar to those obtained earlier on this glass tested in nitrogen gas¹ and in other alcohols^{3,4}. In regions I and II, crack velocity is observed to decrease as the amount of water in the alcohols is decreased. In region III, the data for the butyl alcohol appears to

approach a common curve, as it does for nitrogen gas¹. Hence the mechanisms for fracture of soda lime silica glass in ethyl and butyl alcohols are probably identical to those observed in nitrogen gas and in long chain alcohols studied earlier by Freiman³ and Richter⁴.

The crack growth data from region I of the present paper (Figures 2 and 3) can be compared with earlier data collected in nitrogen gas¹ by plotting the logarithm of the crack velocity as a function of the logarithm of the relative humidity of the water in the alcohol. To do this, crack velocities were taken from Figures 2 and 3 for an applied stress intensity factor of $0.563 \text{ MPa}\cdot\text{m}^{1/2}$, which is the same value of K_{I} used in the earlier study.* The relative humidities were determined from the concentrations of water in the alcohols, using experimental phase diagrams^{7,8}. The resultant plot, Figure 4, indicates a relationship between crack velocity and relative humidity that is roughly linear over the range of relative humidities studied. Furthermore, the alcohol data are found to lie relatively close to the earlier data collected in nitrogen gas. Since the scatter of crack growth curves obtained by the double cantilever beam technique can be as much as a factor of $\sqrt{2}$ along the velocity axis, the difference between the three sets of data can be attributed to experimental scatter. A comparison of the

* This procedure necessitated a linear extrapolation of the region I v - K_{I} data for the butyl alcohol (Figure 3) slightly beyond the range of the data in region I.

ethyl and butyl alcohol data with crack growth data collected by Freiman³ on long chain alcohols was also made; agreement between the two sets of data was similar to that shown in Figure 4. These results confirm earlier conclusion that crack growth in region I is controlled by the relative humidity (i.e. partial pressure) of the environment in contact with the crack tip.^{1,3} As will be discussed in section 4.1, such behavior is consistent with reaction rate theory, in which the effect of environment on the crack growth rate depends on the chemical potential or activity of the water in the alcohol.

In contrast to the results presented above, crack growth in region II does not appear to be controlled directly by the relative humidity of the water in the alcohol. This conclusion is supported by plotting the region II crack growth data presented in Figures 2 and 3 as a function of relative humidity of water in the alcohol. Data plotted in this manner are compared in Figure 5 with similar data obtained by Freiman from studies of crack growth in octyl alcohol³. To assure ourselves that the two sets of data were consistent, new crack growth data were collected in nominally saturated octyl alcohol. The crack velocity in region II for the octyl alcohol was found to be in line with the earlier data by Freiman. A comparison of the data collected in ethyl alcohol and butyl alcohol with the data collected in octyl alcohol shows that the ethyl and butyl alcohol data lie far from the curve obtained for the octyl alcohol. Since the separation of the data is much greater than can be explained by experimental scatter, we conclude that factors other than the relative humidity of water control crack growth in region II.

The conclusion stated above is supported by the double torsion studies (relaxation method) conducted in saturated alcohols, Figure 6. With the exception of the octyl alcohol, which was not fully saturated, the crack velocity in region II is observed to decrease as the chain length of the alcohol is increased. This decrease in velocity correlates directly with the concentration of water in these alcohols, and inversely with the viscosity of the alcohols. Since the alcohols used to obtain Figure 6 were fully saturated (with the exception of the octyl alcohol), they had the same relative humidity of water as the water with which they were in contact. The change of crack velocity of approximately 1.5 orders of magnitude in region II, therefore, cannot be explained by a variation in the relative humidity of the water in the alcohol solutions. A model will be presented in Section 4.3 of this paper, which explains region II crack growth behavior in terms of water concentrations and viscosity of the water-alcohol solution.

The data obtained in region III by the double torsion technique (relaxation method) is presented in Figure 7, for methyl, amyl and decyl alcohol. In agreement with other studies^{3,4}, our data shows a small, but systematic shift of the crack propagation curve to higher values of K_I as the length of the alcohol chain is increased. Furthermore, regardless of alcohol chain length, the curves obtained in alcohol had slopes that were less than those obtained in dry nitrogen gas.

The most surprising aspect of the data shown in Figure 7 has to do with the position of the crack growth curve obtained in decyl alcohol.

Three separate runs using this alcohol resulted in data that were similar to that shown in Figure 7. In all cases, the crack growth curve in decyl alcohol crossed the curve obtained in nitrogen gas, suggesting that at higher crack growth rates, decyl alcohol was retarding the crack growth. This finding, and the observation of a systematic shift and a lower slope of the crack growth data in the alcohols suggests that the alcohols are involved in some intimate way with the fracture process in region III. To further check the possibility of an intimate interaction between organic fluids and the silica network of the glass, experimental data were collected on silica glass in octyl alcohol. The results of this study are shown in Figure 8. If silica were tested in nitrogen gas, it would not have been possible to obtain crack growth data in region III since fracture occurs abruptly in vitreous silica once the crack has passed from region II.⁶ The fact that region III crack growth was obtained in octyl alcohol supports our contention of a direct effect of the alcohol on the fracture process of glass.

To substantiate the data shown in Figure 7, data were obtained using the double torsion technique, constant displacement rate method. The data obtained in this way (Figure 9) support the data shown in Figure 7; the slope of the curve obtained in dry nitrogen, or in decyl alcohol is greater than that obtained in methyl alcohol. Furthermore, the data for decyl alcohol and nitrogen gas fall in a significantly higher range of K_I than the data for methyl alcohol. It is interesting to note that the data for decyl alcohol also falls in a higher range of K_I than that for nitrogen gas, a finding that is consistent with the

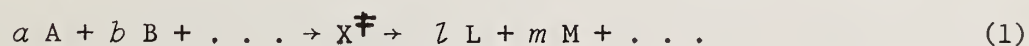
data in Figure 7. However, because of the experimental scatter in both the nitrogen gas and decyl alcohol curves this difference in location cannot be construed as being significant from this figure alone. Finally, data obtained in acetonitrile also had a slope that was significantly lower than that obtained in nitrogen gas, whereas the slope of the curve obtained in heptane was similar to that of nitrogen gas.

4.0 Discussion of Results

4.1 Reaction Rate Theory

The results presented in this paper can be understood in terms of chemical reaction rate theory, which has been used recently by Wiederhorn, Fuller and Thomson¹³ to derive a model for crack growth in ceramics and glasses. To ease our discussion of the present set of data, a brief review of the model is presented in this section, giving the underlying theory and the equations that are pertinent to the results. In Section 4.4, the model is extended to account for electrostatic interactions that are believed to occur between the environment and charges that form during rupture of Si-O bonds at the crack tip.

Consider a chemical reaction of the general type:



If the reverse reaction is negligible, the rate of reaction is given by:

$$\text{Rate} = k_r [A]^a [B]^b \dots \quad (2)$$

where $[A]$, $[B]$, \dots are the concentrations of the reactants. The order of the reaction with regard to each component is given by the exponents in equation 2 (i.e. the order with regard to A is a), and the overall order of the reaction is given by the sum $a + b + \dots$. The reaction rate constant, k_r , can be determined by transition rate theory and is given by the following relation: ^{14,15}

$$k_r = \kappa (kT/h) \exp(-\Delta G_o^\ddagger / RT) (f_A^a f_B^b \dots / f^\ddagger) \quad (3)$$

where κ is the transmission coefficient and is usually assumed equal to 1; ΔG_o^\ddagger is the Gibbs free energy of activation; and f_A , f_B , \dots , f are the activity coefficients for the reactants and for the activated state. The Gibbs free energy of activation is the standard Gibbs free energy change associated with the activation process, and can be related to the standard chemical potentials of the reactants and the activated complex. ^{14,15,16}

$$\Delta G_o^\ddagger = \mu_o^\ddagger - \mu_{Ao}^a - \mu_{Bo}^b - \dots \quad (4)$$

By combining equations 2 and 3, and by using the definition of chemical activity ($a_A = [A] f_A$), the rate of chemical reaction can be

expressed in terms of the chemical activity of the reactants:

$$\text{Rate} = (\kappa/f^\ddagger) (kT/h) a_A^\alpha a_B^b \dots \exp(-\Delta G_O^\ddagger/RT) \quad (5)$$

where a_A , a_B , . . . are the chemical activities of reactants A, B, etc.

Equation 5 can also be expressed in terms of the chemical potential, μ_A , μ_B , . . . , of the reactants:

$$\text{Rate} = (\kappa/f^\ddagger) (kT/h) \exp(a\mu_A + b\mu_B + \dots - \mu_O^\ddagger)/RT \quad (6)$$

where the chemical potentials of the reactants, μ_A , μ_B , etc., are given by the following type of relation: $\mu_A = \mu_{A0} + RT \ln a_A$. The free energy change in the exponent of equation 6 includes effects of chemical composition on reaction rate. By contrast, compositional effects on reaction rate are included in the activities of equation 5.

For purposes of this paper, the crack growth rate is assumed to be proportional to the rate of chemical reaction of the crack tip, and the reaction is assumed to be first order with respect to the water in solution.* For these conditions, equations 5 or 6 can be written as:

* The assumption of a first order reaction may not be valid for very low activities of water. In an earlier study¹, it was noted that the slight curvature of the data for nitrogen shown in Figure 4 suggested a change in the order of the chemical reaction from first order at high relative humidities to one-half order at low relative humidities. This observation was later substantiated for long chain alcohols by Freiman.³ At the high humidities used in the present paper, the data for ethyl and butyl alcohols can be represented by a first order reaction of the water in solution with the glass.

$$v = v_o a_s \exp (\mu_{so} + \mu_g - \mu_o^\ddagger) / RT \quad (7)$$

where a_s is the activity of the water in solution, and where μ_{so} , μ_g and μ_o^\ddagger refer respectively to the water in solution, the reactive species in the glass (presumably Si-O bonds) and the activated complex. The standard state for the water is taken as pure water in the liquid state at 1 atmosphere pressure and a temperature of 25° C, a convention that follows the practice used in references 7 and 8. The frequency factor, kT/h , the transmission coefficient, κ , the activity coefficient, f^\ddagger , and geometric factors relating the number of bonds broken to the crack velocity are all incorporated into v_o of equation 7. It is worth noting that the dependence of crack velocity on the amount of water in the environment is all contained in the activity a_A , whereas the dependence of crack velocity on stress is all contained within the exponent of equation 7.

Although the free energy of activation in equation 7 contains three terms ($\Delta G^\ddagger = \mu_o^\ddagger - \mu_g - \mu_{so}$), these terms are not all equivalent with regard to water enhanced crack growth. The chemical potentials of both the glass, μ_g , and the activated state, μ_o^\ddagger , depend on the state of stress at the crack tip, and hence, are the prime determinants of the slope of the $v-K_I$ curves shown in Figures 1-3. As the stress applied to the crack tip is increased, $\mu_o^\ddagger - \mu_g$ must decrease to account for an increase in the rate of crack growth. The slope of the $v-K_I$ curve depends on the sensitivity of $\mu_o^\ddagger - \mu_g$ to the applied stress, the greater the sensitivity, the steeper the slope of the $v-K_I$ plot. By contrast

the chemical potential of the water does not depend on the state of stress at the crack tip, and hence, has no effect on the slope of the $v-K_I$ curve. It is for this reason that all of the curves in region I of Figures 1-3 have approximately the same slope.

A quantitative treatment of the dependence of applied stress on ΔG^\ddagger has been developed by modelling the crack tip as an elliptical slit in a continuum.¹³ The chemical reaction is assumed to occur at the tip of the slit and the individual bonds at the crack tip are assumed to be acted upon by stresses calculated from the Inglis relation.¹⁷ The following expression is obtained for the free energy of activation:¹³

$$\Delta G^\ddagger = -T\Delta S^\ddagger + \Delta E^\ddagger - [2 K_I / (\pi\rho)^{1/2}] \Delta V^\ddagger - (\gamma^\ddagger V^\ddagger - \gamma V) / \rho \quad (8)$$

where ΔS^\ddagger , ΔE^\ddagger and ΔV^\ddagger are, respectively, the activation entropy, the activation energy and the activation volume. The parameter ρ is the radius of curvature of the crack tip, and is assumed to be of the order of the lattice, or network spacing in the solid: 0.5 nm for glass.*

The term containing K_I on the right hand side of the equation is the stress to which the reacting species at the crack tip are subjected. This portion of the activation free energy determines the stress dependence of crack growth rate. More specifically, if crack growth data are fitted to the following empirical relation:

* A curved crack tip is assumed primarily to estimate the stress level at the crack tip. The nature and structure of real crack tips in glass are, at present, not fully understood.

$v = v_o \exp (-E^* + bK_I)/RT$, then the slope of the v - K_I data, b , can be used to determine the activation volume for crack growth. Equating b to the coefficient of K_I in equation 8, the following relation is obtained for ΔV^\ddagger :

$$\Delta V^\ddagger = (b/2) (\pi\rho)^{1/2} \quad (9)$$

This expression will be used later in the paper to relate the crack growth data (i.e. the slope b) to a variable calculated from an electrostatic model of environmental interactions at crack tips.

The last term on the right hand side of equation 8 is included to account for the fact that surface curvature can modify the chemical potential of the reacting species.¹³ The parameters γ and V are the surface tension and molar volume of the reacting species (the strained Si-O bonds of glass for example) before reaction, while γ^\ddagger and V^\ddagger are these same quantities for the activated complex on surface during reaction. The inclusion of this surface energy term follows the approach first taken by Charles and Hillig¹⁸ in their dissolution model of static fatigue.

4.2 Region I Crack Growth

The crack growth data collected in the present paper can best be compared with equation 7 of the theory presented in Section 4.1. Since v_o and the chemical potentials μ_{so} , μ_g and μ_o^\ddagger are constants for a given temperature and state of stress, the equation implies that at a constant applied stress intensity factor, the crack velocity will depend only on

the activity, a_s , of water in the alcohol solution. If the standard state of the chemical potential of the water in the alcohol is taken as pure water, then the chemical activity of the fully saturated alcohols used in the present studies is ≈ 1 , at saturation, (i.e. the chemical potentials of the water are almost the same for all of the alcohols). Furthermore, if water vapor at room temperature is assumed to behave as a perfect gas, then the activity of the water is given by the ratio of the partial pressure, p_s , of water over the solution to that, p_{s0} , over pure water: $a_s = p_s/p_{s0}$.¹⁶ Since p_s/p_{s0} is defined as the relative humidity, the crack velocity is predicted to be proportional to the relative humidity of the water, as is observed experimentally (Figure 4). Hence we conclude that the chemical activity, or what is equivalent, the chemical potential of water in solution is the prime driving force for crack growth in region I.

The above observation has rather broad implications with regard to the effect of water on the lifetime of structural ceramics. As long as the chemical potential of water is the same in two solutions, the response of cracks in structural ceramics to stress will be identical with regard to region I crack growth. Since the lifetime of ceramics is controlled mainly by region I (i.e. slow) crack growth, the chemical potential of water in solution is the prime environmental determinant of structural reliability. Although several investigations of the effect of relative humidity on component lifetime are consistent with this prediction,^{19,20} this subject has not been studied systematically and certainly warrants further investigation.

4.3 Region II Crack Growth

The mechanism described in Section 4.1 will control crack growth as long as the number of water molecules reaching the crack tip maintains the activity of water at the crack tip constant. When the velocity is fast enough, the water will be used up at a rate faster than can be supplied by diffusion from the environment. When this happens, the rate of transport will control the rate of crack motion.

Using a one dimensional model of diffusive transport of water to a crack tip it has been shown that the rate of crack growth in region II can given by:¹

$$v = 0.0275 D X_o / n\delta \quad (10)$$

where D is the diffusivity of water in the alcohol, δ is the diffusive boundary layer thickness in front of the crack tip, X_o is the molar concentration of the water in the solution and n is the order of the chemical reaction.* For relative humidities >0.1 , the parameter n has been shown to be 1 for water reactions in nitrogen gas and will be assumed to be equal to 1 for the alcohols.

* The constant 0.0275 is appropriate when all variables in equation 10 are expressed in SI units.

The diffusivity, D , of water in alcohols has been measured in only a few of the shorter chain length alcohols.²¹ Hence in order to compare the data with equation 4, it is necessary to use a theoretical expression for the diffusion coefficient. For this purpose we use the Stokes-Einstein relation:²²

$$D = (kT)/(6\pi r\eta) \quad (11)$$

where η is the fluid viscosity, r is the radius of the diffusing molecule and k is the Boltzman constant. Substituting equation 11 into equation 10, the following equation is obtained for the crack velocity in region II:

$$v = (0.0275 kT/(6\pi r\delta))(X_o/\eta) \quad (12)$$

If the form of equation 12 is correct, then the crack velocity in region II should be proportional to X_o/η (i.e. the ratio of the molar concentration of water in the alcohol to the viscosity of the alcohol). The data plotted in this manner (Figure 10) scatters about a line of slope 1, as would be expected from the theory. Much of the scatter in Figure 10 can be attributed to the uncertainty in selection of the characteristic velocity of region II. As can be seen from examination of Figure 6, the error in estimating the crack velocity in region II can be as much as a factor of 2. Furthermore, the fact that crack velocity in region II exhibits a small but significant dependence on applied stress intensity factor contributes to the uncertainty in selecting

characteristic velocities. Considering these sources of scatter in the experimental data, the correlation between the variables shown in Figure 10 lends credence to our model of diffusion controlled crack growth.

The data shown in Figure 10 can be used to obtain an estimate of the diffusive boundary layer, δ , at the crack tip. The intercept on Figure 10 is approximately 2.5×10^{-8} m/s; substituting this value of crack velocity into equation 12 and assuming $T = 300$ K and r (the molecular radius of H_2O) = 0.3 nm a value of $\delta = 0.8$ μ m is obtained. This value is approximately one-third that obtained in earlier studies of crack growth in nitrogen gas. Since the collision distances in liquids (~ 0.5 nm) are less than the collision distances in gases (~ 50 nm at standard temperature and pressure), the boundary layer, δ , in a liquid is expected to be less than that in a gas. The thickness of the boundary is likely to vary from one type of liquid to another, depending on the nature of the interactions that occur between the liquid and the water that is dissolved in it.

4.4 Region III Crack Growth

The data presented in this paper and in the papers by Freiman³ and Richter⁴ suggest that alcohols and other organic liquids affect crack growth in Region III. The influence of these environments is indicated by small shifts in the position of the crack propagation curves and by small decreases in the slopes of these curves when compared to the

position and the slope of the curve obtained in nitrogen gas. Two possible mechanisms were considered to explain our experimental observations. The first involves viscous drag of the liquid on the freshly formed fracture surfaces, which would retard crack growth, causing small shifts in the crack velocity curves. If viscous drag were an important mechanism, then the crack growth curve would be expected to shift to higher values of K_{I} as the viscosity of the liquid increased. This type of shift in the position of the crack growth curve is in fact observed for the alcohols. The possibility of a viscous drag contribution to the crack growth behavior was, however, rejected for two reasons: (1) the shape of the crack growth curves obtained experimentally differs from that predicted from fluid dynamic equations; (2) viscous drag cannot explain the experimental crack growth behavior at low velocities, since all of the crack growth curves would be expected to join up with the nitrogen curve as the viscous drag effects vanished. To support these conclusions, detailed discussion of viscous drag is given in Appendix A.

The second mechanism considered to explain our experimental findings involves electrostrictive interactions between the glass and the fluid at the crack tip. If one accepts the chemical interaction model of subcritical crack growth in ceramic materials, then the slope of the crack propagation curves in regions I or III is determined by the activation volume, ΔV^{\ddagger} , of the chemical reaction that occurs at the crack tip.¹³ When fracture is caused by the reaction of water with glass, ΔV^{\ddagger} represents the difference in molar volume between the

reactants and the chemical complex in the activated state. If fracture occurs in the absence of water, ΔV^\ddagger then represents the change in volume that occurs as the strained Si-O bonds move into an activated state. Referred to as a fission reaction in the chemical literature, this is the type of reaction of primary interest in fracture processes.

When a fission reaction occurs in a liquid environment, it has been shown that the activation volume normally consists of two parts: one part relates to the stretching of the bond that is being broken; the second part relates to volume changes in the fluid surrounding the reacting molecule.^{15,23-25} The second part is usually attributable to electric charge formation or destruction during the chemical reaction, which results in a localized electrostriction, and hence a change in volume in the fluid surrounding the reacting species. This change in volume must be included as part of the activation volume because the volume change is concomitant with the fission reaction. For normal chemical reactions, charge formation or destruction results in rather large contributions to the activation volume. In fact, the electrostatic portion of the activation volume is usually 3 to 10 times that due to changes in bond length alone. Hence, if charges are either formed or destroyed during the rupture of a silicon-oxygen bond in glass, electrostatic effects in the glass during crack growth will have to be considered.

In order to model the effect of environment on a fission reaction in glass, a procedure similar to that used by Wiederhorn, Fuller and Thomson¹³ is employed. The procedure models the crack tip as an ellipse and uses the stress at the major axis of the ellipse, calculated from the Inglis relation,¹⁷ as the driving force for the chemical reaction. The crack tip stress then replaces pressure as the thermodynamic parameter usually used to discuss chemical reactions. The crack tip stress is of course a negative pressure. The effect of charge formation is then treated by elementary solvation theory:^{16,22} the charged atoms or molecules formed during the reaction being approximated by charged conducting spheres; the medium surrounding the reacting species being treated as a continuum with a dielectric constant, ϵ . For the fission of a silicon-oxygen bond during crack growth in glass, positive and negative charges are assumed to form on the silicon and oxygen atoms respectively as they are separated. This assumption that a full unit of charge develops during the activated state is based on the work of Akmed et al.,²⁴ who reported charge formation on silicon and oxygen atoms during the crushing of silica glass. Suggestions of charge formation during fracture were also made in earlier glass literature.^{27,28}

The procedure used in the present paper to estimate the electrostatic component of the activation volume differs somewhat from that used by Wiederhorn, Fuller and Thomson,¹³ in that the reacting species (the oxygen and the silicon) are assumed to lie at a stressed surface of the glass. This assumption is necessary in order to evaluate the effect of environment on the reacting species. Furthermore, we assume

that the electrostatic component of the activation volume (or activation free energy) is entirely the result of charging the oxygen and silicon atoms during the fission process. Finally, we assume that the reaction is sufficiently slow that the static component of the dielectric constants can be used to estimate the electrostrictive processes at the crack tip, and that both the glass and the environment at the crack tip can be treated as a continuum. These last two assumptions are usually made to treat the kinetics of chemical reactions in liquids.^{15,23-24}

A schematic diagram of the model used in the present paper to account for the electrostatic component of the activation volume is given in Figure 11. Charges are assumed to form at a flat interface during the reaction. Each Si and O atom in the activated state is assumed to react independently with the glass and the surrounding environment during the fission reaction. This assumption is often made in evaluating the electrostatic component of the activation volume and tends to neglect dipole or quadrupole effects on reaction rate. The configuration shown in Figure 11 was chosen because electrostatic effects of the dielectric fluid on the rupture process are easily estimated from this model. The model does not take into account effects that result from curvature of the crack near the crack tip or steric hinderance due to limits in the dimensions of the crack near its tip. It is assumed that the change in free energy, ΔG_{es} , when a charge forms at the interface can be estimated by the energy required to charge conducting spheres of radius, r_{Si} and r_O , equal to the radius of the silicon and oxygen atoms (0.04 and 0.14 nm) respectively. Each atom is assumed to develop a full unit of charge as rupture occurs,

a positive charge for the silicon atom and a negative charge for the oxygen atom. The free energy of formation of each charged atom, ΔG_{es} , is given by:^{*}

$$\Delta G_{es} = (N_a e^2/r)/(\epsilon_1 + \epsilon_2) \quad (13)$$

per mole of charge formed for each ion. N_a is Avogadro's constant, and ϵ_1 and ϵ_2 are the dielectric constants of the glass and the liquid respectively.

The electrostatic component of the activation volume for the reaction is determined from equation 13, using the relation, $\Delta V_{es} = \partial \Delta G_{es} / \partial P$, where P is the pressure that constrains the chemical reaction. When the reaction occurs at the surface of the glass, this pressure is equal to the negative of the crack tip stress. Hence for a chemical reaction constrained by a pressure, P, the activation volume ΔV_{es} is given by:

$$\Delta V_{es} = (N_a e^2/r) [-(\epsilon_1 + \epsilon_2)^{-1} \partial \ln r / \partial P - (\epsilon_1 + \epsilon_2)^{-2} \partial \epsilon_1 / \partial P] \quad (14)$$

for each ion. The derivation of equation (14) is based on the assumption that the pressure is applied only to the glass, hence the partial derivative is taken only with regard to ϵ_1 . Equation 14 can be written in terms of the bulk modulus B:

$$\Delta V_{es} = (N_a e^2/r) [(3B)^{-1} (\epsilon_1 + \epsilon_2)^{-1} - (\epsilon_1 + \epsilon_2)^{-2} \partial \epsilon_1 / \partial P] \quad (15)$$

^{*}This equation is derived in Appendix B.

From equation 15, we note that the electrostatic contribution to the activation volume depends on four parameters: the size of the electrostatic charge formed during the reaction; the value of the bulk modulus; the value of the dielectric constants (ϵ_1 and ϵ_2) and the partial derivative of the dielectric constant with regard to the applied pressure. As already mentioned, equation 15 neglects any dipole, or quadrupole contributions to ΔV_{es} . The partial derivative of ϵ_1 with regard to P is usually negative for solids; however, some positive values have been measured.^{29,30} When $\partial\epsilon_1/\partial P$ is negative, then the activation volume is positive. However when $\partial\epsilon_1/\partial P$ is positive, the activation volume, ΔV_{es} , can be positive or negative depending on the size of the two terms in the square brackets. Finally, the dependence of ΔV_{es} on environment depends primarily on the dielectric constant, ϵ_2 , of the environment.

Crack growth data can be compared with the electrostrictive model for crack growth by plotting ΔV^\ddagger , the total activation volume (equation 9), as a function of ΔV_{es} , the electrostatic portion of the activation volume. It is worth noting that ΔV^\ddagger determined from equation 9 contains both the stretching and the electrostatic components of the activation volume. For crack growth studies conducted on soda-lime-silica glass in different environments, ΔV_{es} is expected to depend primarily on ϵ_2 , the dielectric constant of the fluid at the crack tip. For fluids that have a high dielectric constant (i.e. water, formamide) ΔV_{es} is expected to be small, and as a consequence, the value obtained for ΔV^\ddagger will be due primarily to stretching of the Si-O bonds by the applied forces. For

environments that have low dielectric constants (i.e. alkanes, vacuum) ΔV_{es} will be large and ΔV^\ddagger will contain components due both to electrostatic interactions and to stretching. Figure 12 presents a plot of ΔV^\ddagger as a function of ΔV_{es} .^{*} Despite the experimental scatter, a correlation between ΔV^\ddagger and ΔV_{es} is apparent from the figure. The figure demonstrates a definite dependence of crack growth data on the dielectric constant of the test media, and as such lends support to the idea that electrostatic interactions between the environment and the highly strained bonds at the crack tip influence crack growth. The scatter of the data in Figure 12, illustrates the difficulty of obtaining accurate values of the slope of the $v-K_I$ data in region III, especially when the slopes are high, as they are in alkanes, nitrogen gas, and vacuum. Further confirmation of the theory will require the development of more accurate methods of determining the slope of crack growth curves. These techniques should then be applied to crack growth

* The authors could find no values of $\partial \epsilon_1 / \partial p$ in the literature for soda-lime-silica glass. The value of $\partial \epsilon_1 / \partial P$ ($-9.72 \times 10^{-11} \text{ Pa}^{-1}$) used for Figure 12 was obtained by Colwell³⁰ on an alkali containing glass made at the National Bureau of Standards. The fluid dielectric constants ϵ_2 and the slopes, b , of the crack growth curves used for Figure 12 are given in Table 2.

studies in low dielectric constant liquids, $\epsilon < 8$, where electrostatic effects are expected to be greatest. Furthermore, a variety of glasses and single phase ceramics should be studied to evaluate the effect of $\partial\epsilon_1/\partial P$ on crack growth data.

5. Summary

This paper presents the results of a series of studies to determine the effect of water and a variety of organic liquids on crack growth in soda-lime-silica glass. Throughout the paper the crack growth process is viewed as a chemical reaction and the data are interpreted in terms of chemical reaction rate theory. In the presence of a chemically active environment, rupture of the Si-O bonds of the glass network is viewed as a fission reaction in which Si-O bonds, strained by the crack tip stresses, are cleaved by the chemical environment. In the absence of a chemical reaction between the glass and the environment the fission reaction occurs as a result of a stress induced cleavage of the Si-O bonds of the glass network structure. The three regions of crack growth, observed in crack growth studies are interpreted in terms of reaction rate theory.

In region I, crack growth in organic liquids is the result of a chemical reaction between the active component in the environment (usually H₂O) and the glass; the rate of growth is controlled by the chemical potential of the active component. This finding confirms those of earlier studies and is consistent with the chemical reaction rate

theory of crack growth. In region II the rate of crack growth is determined by diffusion of the reactant to the crack tip. We show that crack growth in region II is not controlled by the chemical potential of the reactant, but by its concentration. Using the Stokes-Einstein relation for the diffusivity, a linear relation is obtained between the crack velocity and the ratio of the concentration of water to the viscosity of the organic fluid. Finally in our discussion of crack growth in region III, we introduce the idea that electrostrictive effects at crack tips can influence the crack growth behavior of solids. The concept of an electrostatic component to the activation volume is commonly used by physical chemists to explain the effects of solvents on rates of chemical reactions. In this paper, a model was developed to quantify the effect of dielectric media on crack growth rate in glass. The model follows classical chemical lines and has the virtue of providing a relation between the slope of $v-K_I$ data and the dielectric constants of the glass and the test medium. A plot of the total activation volume obtained from the slope of crack growth data versus the electrostatic component of the activation volume calculated from theory, lends support to the model and suggests that electrostrictive effects influence the growth of cracks in glass. Despite this agreement, the approximate nature of the model should be recognized. Further studies may show that some variables neglected in the model are in fact important to our understanding of region III crack growth. Clearly, additional data is needed to fully evaluate the theory presented in this paper.

Acknowledgment: This work was supported by the Office of Naval Research, Metallurgy and Ceramics Program. The authors are grateful for the technical assistance of A.C. Gonzalez, D. Kravitz, and G.S. White. Helpful discussions with R. M. Thomson, J. W. Cahn, B. R. Lawn and H. Richter are also gratefully acknowledged.

REFERENCES

1. S. M. Wiederhorn, "Influence of Water Vapor on Crack Propagation in Soda-Lime Glass", *J. Am. Ceram. Soc.*, 59, 407-414 (1977).
2. K. Schonert, H. Umhauer and W. Klemm, "The Influence of Temperature and Environment on the Slow Crack Propagation in Glass", pp 474-482 in *Proc. 2nd Int. Conf. on Fracture, Blythen, 1969*, Chapman and Hall, London (1970).
3. S. W. Freiman, "Effect of Alcohols on Crack Propagation in Glass," *J. Am. Ceram. Soc.* 57, 350-353 (1974).
4. H. Richter, "The Effect of Different Liquids on the Transition from Slow to Fast Crack Propagation in Soda-Lime-Glass," pp 618-624 in *The Physics of Non-Crystalline Solids*, G. H. Frischat, ed., *Trans. Tech. Publications*, CH-4711 Aedermansdorf, Switzerland (1977).
5. C. L. Quackenbush and V. D. Frechette, "Crack-Front Curvature and Glass Slow Fracture," *J. Am. Ceram. Soc.* 61, 402-406 (1978).
6. S. M. Wiederhorn, H. Johnson, A. M. Diness and A. H. Heuer, "Fracture of Glass in Vacuum," *J. Am. Ceram. Soc.*, 57, 336-341 (1974).
7. M. Randall and H. P. Weber, "The Activity of the Constituents in Mixtures of n-butyl Alcohol and Water at 30 °C," *J. Phys. Chem.* 44, 917-920 (1940).
8. H. R. Null, *Phase Equilibrium in Process Design*, Wiley-Interscience, New York (1970).
9. S. M. Wiederhorn, "Subcritical Crack Growth," pp 613-646 in *Fracture Mechanics of Ceramics, 2, Microstructure Materials and Applications*, R. C. Bradt, D. P. H. Hasselman, and F. F. Lange, eds., Plenum Press, New York (1974).
10. B. J. Pletka, E. R. Fuller, Jr., and B. G. Koepke, "An Evaluation of Double-Torsion Testing-Experimental," pp 19-37 in *Fracture Mechanics Applied to Brittle Materials*, ASTM STP 678, S. W. Freiman, ed., American Society for Testing and Materials (1979).
11. T. A. Michalske and V. D. Frechette, "Dynamic Effects of Liquids on Crack Growth Leading to Catastrophic Failure in Glass," *J. Am. Ceram. Soc.*, 63, 603-609 (1980).
12. S. W. Freiman, D. R. Mulville, and P. W. Mast, "Crack Propagation Studies in Brittle Materials", *J. Mat. Sci.* 8, 1527-33 (1973).
13. S. M. Wiederhorn, E. R. Fuller, Jr., and R. Thomson, "Micromechanisms of Crack Growth in Ceramics and Glasses in Corrosive Environments," *Metal Science* 14, 450-458 (1980).

14. S. Glasstone, K. J. Laidler, and H. Eyring, Theory of Rate Processes, McGraw-Hill, New York, 1941.
15. G. Kohnstam, "The Kinetic Effects of Pressure," pp 355-408 in Progress in Reaction Kinetics, G. Porter, ed., Pergamon Press, London (1970).
16. W. J. Moore, Physical Chemistry, Prentice-Hall Inc., Englewood Cliffs, N.J. (1972).
17. C. E. Inglis, "Stresses in a Plate due to the Presence of Cracks and Sharp Corners," Trans. Inst. Naval Archit. 55, 219- (1913).
18. R. J. Charles and W. B. Hillig, pp 511-27 in Symposium on Mechanical Strength of Glass and Ways of Improving It. Florence, Italy, September 25-29, 1961. Union Scientifique Continentale du Verre, Charleroi, Belgium, 1962.
19. R. E. Mould, "Strength and Static Fatigue of Abraded Glass under Controlled Ambient Conditions: IV. Effect of Surrounding Medium," J. Am. Ceram. Soc. 44, 481-91 (1961).
20. J. E. Ritter, Jr., and C. L. Sherburne, "Dynamic and Static Fatigue of Silicate Glasses," J. Am. Ceram. Soc. 54, 601-605 (1971).
21. P. A. Johnson and A. L. Babb, "Liquid Diffusion of Non-Electrolytes," Chem. Rev. 56, 387-453 (1956).
22. J. O'M. Bockris and A. K. N. Reddy, Modern Electrochemistry, vol. 1, Plenum Press, New York (1970).
23. S. D. Hamann, "Chemical Kinetics," pp 163-207 in High Pressure Physics and Chemistry, vol. 2, R. S. Bradley, ed., Academic Press, New York (1963).
24. E. Whalley, "Use of Volumes of Activation for Determining Reaction Mechanisms," Advan. Phys. Org. Chem. 2, 93-162 (1964).
25. C. A. Eckert, "High Pressure Kinetics in Solution," Ann. Rev. Phys. Chem. 23, 239-264 (1972).
26. K. A. Akhmed-zade, V. V. Baptizmanskii, V. A. Zakrevskii, and E. E. Tomashevskii, "Paramagnetic Centers Produced by Mechanical Destruction of Silica," Soviet Physics-Solid State, 14, 351-354 (1972).
27. R. E. Benson and J. E. Castle, "Reactions of Freshly Formed Surfaces of Silica," J. Phys. Chem. 62, 840-843 (1958).
28. W. A. Weyl, "Crystal Chemical Considerations of the Surface Chemistry of Silica," Research 3, 230-235 (1950).

29. R. S. Bradley, "Other Miscellaneous Effects of Pressure," pp 325-337 in High Pressure Physics and Chemistry, vol. 2, R. S. Bradley, ed., Academic Press, New York (1963).
30. J. H. Colwell, "Stable Pressure Transducer," National Bureau of Standards Report, NBSIR 76-1116, July 1976.
31. S. M. Wiederhorn and L. H. Bolz, "Stress Corrosion and Static Fatigue of Glass," J. Am. Ceram. Soc. 53, 543-548 (1970).
32. S. W. Freiman, "Effect of Straight-Chain Alkanes on Crack Propagation," J. Am. Ceram. Soc. 58, 339-340 (1975).
33. S. W. Freiman, "Temperature Dependence of Crack Propagation in Glass in Alcohols," J. Am. Ceram. Soc. 58, 340-341 (1975).
34. P. C. Paris and G. C. Sih, "Stress Analysis of Cracks" in Fracture Toughness Testing and Its Applications, ASTM STP 381 (1965), pp 80-81.
35. G. I. Barenblatt, "The Mathematical Theory of Equilibrium Cracks in Brittle Fracture," Adv. Appl. Mech. 7, 55-126 (1962).
36. G. K. Batchelor, An Introduction to Fluid Dynamics, Cambridge University Press, Cambridge (1967).
37. I. S. Gradshteyn and I. M. Ryzhik, Table of Integrals, Series, and Products (Academic Press, New York, 1980), p. 527 (formula 4.224.11).
38. J. D. Jackson, Classical Electrodynamics (John Wiley & Sons, Inc. New York, 1962).

APPENDIX A

The Effect of Viscous Flow on Crack Motion

In an earlier section of this paper, the idea that the position of the $v-K_I$ curves in alcohol could be explained by viscosity effects was rejected. In this section we develop equations that relate the crack motion to the viscosity of the fluid at the crack tip and show why the idea was rejected.

Assume that the crack can be represented by a parabola that intersects an external surface, Figure 1A. The parabola is selected because the crack has the shape of a parabola near its crack tip in the linear elastic approximation. The crack length is equal to c , the y -coordinate is perpendicular to the plane of the crack and the x coordinate lies in the plane of the crack. As the crack moves along, it sucks fluid into the crack opening, which is exposed to an infinite reservoir of fluid at an ambient pressure, P_a . In order for the fluid to flow to the crack tip, the fluid pressure decreases from the crack opening to the crack tip. Therefore the fluid within the crack is at a negative pressure relative to the ambient pressure, P_a . The negative pressure loads the surface of the crack in such a way as to tend close the crack. Thus, the closing force on the crack surface produces a negative stress intensity factor, K_p which opposes the positive, applied stress intensity factor, K_a , that is driving the crack to propagate.

To calculate the decrease in pressure from the crack opening to the crack tip, and to estimate the negative stress intensity factor, we assume that the coordinate system is fixed to the crack tip. Then the crack surface appears to recede from the crack tip at a velocity v_o , which is also the velocity of the crack. The half width of the crack, y_o , is determined by the standard (plane strain) fracture mechanics relation for the displacement in the vicinity of a crack that is subject to a stress intensity factor K_I (see, for example, Ref. 34)

$$y_o^2 = [2K_I(1-\nu)/G]^2(x/2\pi) \quad (1A)$$

where G is the shear modulus of the solid and ν is Poisson's ratio. The stress intensity factor, K_I , therefore describes the stresses and displacements at the crack tip and has to be equal to the sum of K_a and K_p : $K_I = K_a + K_p$. This approach to the crack tip stresses is similar to the approach used by Barenblatt³⁵ in his discussion of crack tip forces.

At any distance, x , from the crack tip, the pressure drop across a section, dx , of the crack is given by the Poiseuille flow equation for a parallel sided channel:

$$v_o = (1/3\eta) (dP/dx) y_o^2 \quad (2A)$$

where η is the viscosity of the fluid in the crack. As noted by Batchelor,³⁶ this approximation is valid provided the slope of the

walls of the channel change slowly with distance along the channel. Substituting equation 1A into equation 2A and integrating the pressure drop from a point within the crack to the crack mouth, the following equation is obtained for the pressure, P, at any point within the channel:

$$P = P_a + 6\pi v_o \eta [G/2K_I(1-\nu)]^2 \ln (x/c) \quad (3A)$$

Note that as the position x approaches the crack tip (i.e. $x \rightarrow 0$), large negative pressures occur within the fluid.

The negative stress intensity factor, K_p , that results from the reduction of pressure within the crack can be calculated from a standard equation for a two dimensional crack within a solid that is subject to an applied stress $\sigma(x)$:³⁴

$$K_p = 2 (c/\pi)^{1/2} \int_0^c \sigma(x') dx' / [c^2 - (x')^2]^{1/2} \quad (4A)$$

where $x' = c-x$ measures the distance from the crack mouth.

The stress $\sigma(x')$ at any point on the crack surface is determined from the difference between the pressure within the crack and the external pressure: $\sigma(x') = P - P_a$. Note from 3A that $\sigma(x')$ is a negative quantity, as it should be for a closing force on the crack tip. Substituting the equation for $\sigma(x')$ into equation 4A and integrating,³⁶ the following equation is obtained for K_p :

$$\begin{aligned}
K_p &= -1.5 (\pi \ln 2 + 4C) v_o \eta [G/K_I(1-\nu)]^2 (\pi c)^{1/2} \\
&= -8.76 v_o \eta [G/K_I(1-\nu)]^2 (\pi c)^{1/2} \qquad (5A)
\end{aligned}$$

where $C = 0.915966$ is Catalan's constant.

For a constant crack length, c , K_p depends only on the crack velocity, v_o , and the crack tip stress intensity factor, K_I ; since K_I is a slowly varying function of v_o for ceramic materials, K_p depends primarily on v_o .

Normally when a v - K_I curve is determined experimentally, it is K_a that is measured and presented as a plotting parameter. As long as K_p is small, the v - K_I curve and the v - K_a curve will be indistinguishable. However when K_p becomes large relative to K_a , the experimental curve will diverge from the "true" v - K_I curve. This occurs when part of the applied load is transferred from the specimen to the fluid within the crack. The range of velocities over which this occurs can be calculated by evaluating equation 5A and comparing it with crack tip stress intensity factor. As shown in Table 1A, where $P-P_a$ and K_p are calculated as a function of velocity for water, the transition range over which these viscous effects are important occur over a relatively narrow range of crack velocities. The data in Table 1A are plotted in Figure 2A to give a predicted v - K_a curve. We note that the curve bends over rather

sharply, over a velocity range of about two orders of magnitude. Behavior of this type has been observed for water by Schönert et al.² and by Michalske and Frechette for water and for methyl alcohol.¹² Since the shape of the curves observed in the present paper are not similar to those obtained for the alcohols in region III, we conclude that viscous effects of the crack tip fluid played little if any role in the present experiments, thus justifying our statements in section 4.3.

APPENDIX B

Electrostatic Energy of a Charged Sphere on a Dielectric Interface

The model used in section 4.3 to describe the region III crack growth behavior relates the change in free energy during the crack-tip fission reaction to the electrostatic energy required to charge a conducting sphere embedded on a dielectric interface (see Figure 12). In this appendix we derive an expression for this electrostatic energy.

In a linear dielectric medium, the electrostatic energy of a system of charges is related to the electric field \mathbf{E} that they produce by the relation:³⁸

$$W_{es} = \frac{1}{8\pi} \int \epsilon |\mathbf{E}|^2 d^3R \quad (1B)$$

where ϵ is the dielectric constant and the volume integral is over all space. Accordingly, the problem reduces to finding the electric field \mathbf{E} , or its scalar potential ϕ , since then $\mathbf{E} = -\nabla\phi$, and integrating the results according to Eq. (1B).

The electrostatic potential ϕ is determined as a solution of Poisson's equation:

$$\nabla^2\phi = -4\pi\chi \quad (2B)$$

where χ is the charge density. The boundary conditions for the present problem require: (1) that the surface of the conducting sphere is at a constant potential; (2) that the displacement field, ϵE , normal to the sphere is equal to 4π times the surface charge density; (3) that the surface charge density integrated over the surface of the sphere is Q ; and (4) that the tangential components of E is continuous across all boundaries. Rather than solve Eq. (2B) directly, we note that a solution of Poisson's equation is unique when the potential is specified on all closed conducting surfaces (Dirchlet boundary conditions), as in the present problem. Thus, if we obtain a solution by any means, we have the unique solution.

A solution to the present problem is obtained from the electrostatic potential of a point charge Q embedded on a planar interface between two semi-infinite dielectrics. This solution:³⁸

$$\phi(R) = \frac{2Q}{(\epsilon_2 + \epsilon_1)R} \quad (3B)$$

has spherical equipotential surfaces and hence gives the proper form of the solution for distance greater than the radius r of the conducting sphere (i.e., $R > r$). Inside the sphere the potential is constant:

$$\phi = \frac{2Q}{(\epsilon_2 + \epsilon_1)r}, \text{ for } R \leq r \quad (4B)$$

The electric field vector is given by the negative of the gradient of the potential, and only has a radial component E_R since the potential is spherically symmetric:

$$E_R = \begin{cases} 0 & , \text{ for } R < r \\ \frac{2Q}{(\epsilon_2 + \epsilon_1)R^2} & , \text{ for } r < R \end{cases} \quad (5B)$$

It is easy to verify that this solution satisfies the remaining boundary conditions.

The electrostatic energy required to charge the conducting sphere is obtained by integrating Eq. (5B) in Eq. (1B):

$$\begin{aligned} W_{es} &= \frac{1}{8\pi} \int_{\text{dielectric 2}} \epsilon_2 E_R^2 d^3R + \frac{1}{8\pi} \int_{\text{dielectric 1}} \epsilon_1 E_R^2 d^3R \\ &= \frac{Q^2}{(\epsilon_2 + \epsilon_1)r} \end{aligned} \quad (6B)$$

In section 4.3 the charge Q is taken to be a full unit of electronic charge, $Q = e$.

Table 1: Viscosity, Water Concentration and Relative Humidity of Alcohols used in Region II Crack Growth Study.

Alcohol	Viscosity (Pa·s)	Water Concentration (mol/liter)	Percent Relation Humidity
Butyl	3.13×10^{-3}	9.2	100
Amyl	3.46×10^{-3}	4.08	100
Hexyl	3.95×10^{-3}	3.04	100
Heptyl	5.16×10^{-3}	2.52	100
Octyl	6.31×10^{-3}	1.13	50
Decyl	10.99×10^{-3}	1.68	100
Ethyl (1%)	$1.1 \times 10^{-3*}$	0.555	7
Butyl (0.2%)	$2.95 \times 10^{-3*}$	0.111	5
Butyl (1%)	$2.95 \times 10^{-3*}$	0.555	21
Butyl (5%)	$2.95 \times 10^{-3*}$	2.78	70

* The viscosities of the partially saturated ethyl and butyl alcohols were assumed to be equal to the pure alcohols at 20 °C.

Table 2: A comparison of the slopes, b , of crack growth data with the dielectric constant, ϵ_1 , of the test medium. All crack growth measurements were made on soda-lime-silica glass; slopes were determined from an empirical fit to the equation: $v = v_0 \exp bK_I/RT$.

Test Medium	Dielectric Constant, ϵ_1	Slope, b MKS units	Test Method
Formamide	109	0.168	D.C.B.
Water	78	0.111	D.C.B., ref. 31
Acetonitrile	39	0.232	Double Torsion
Methanol	33	0.182 0.169	Double Torsion Double Torsion
Hexanol	13.3	0.223	D.C.B., ref. 33
Heptanol	12.2	0.283	D.C.B., ref. 33
Octanol	10.3	0.228	D.C.B., ref. 33
Decanol	8.0	0.240 0.252 0.391	D.C.B., ref. 33 Double Torsion Double Torsion
Trichloroethylene	3.4	0.463	D.C.B.
Alkanes	2	0.488	D.C.B., ref. 32
Heptane	2	0.361 0.772 0.724	Double Torsion Double Torsion D.C.B., ref. 32
Nitrogen	1	0.636 0.542 0.823	Double Torsion Double Torsion D.C.B., ref. 1
Vacuum	1	0.88	D.C.B., ref. 6

Table 1A. Effect of viscous forces on crack motion calculated from equations 3A and 5A. The pressure is calculated for a 1 mm crack at a distance of 1 μm from the crack tip. ($G = 28 \text{ GPa}$, $\nu = 0.24$ and $\eta = 1 \text{ mPa}\cdot\text{s}$)

Crack Velocity (m/s)	K_I ($\text{mPa}\cdot\text{m}^{1/2}$)	$P - P_a$ (mPa)	K_P ($\text{mPa}\cdot\text{m}^{1/2}$)
1.00×10^{-1}	0.570	-13.6	-0.205
5.72×10^{-2}	0.560	- 8.1	-0.122
2.63×10^{-2}	0.543	- 3.9	-0.059
1.20×10^{-2}	0.530	- 1.9	-0.028
5.25×10^{-3}	0.505	- 0.91	-0.014
2.40×10^{-3}	0.490	- 0.44	-0.007
1.00×10^{-3}	0.470	-0.20	-0.003

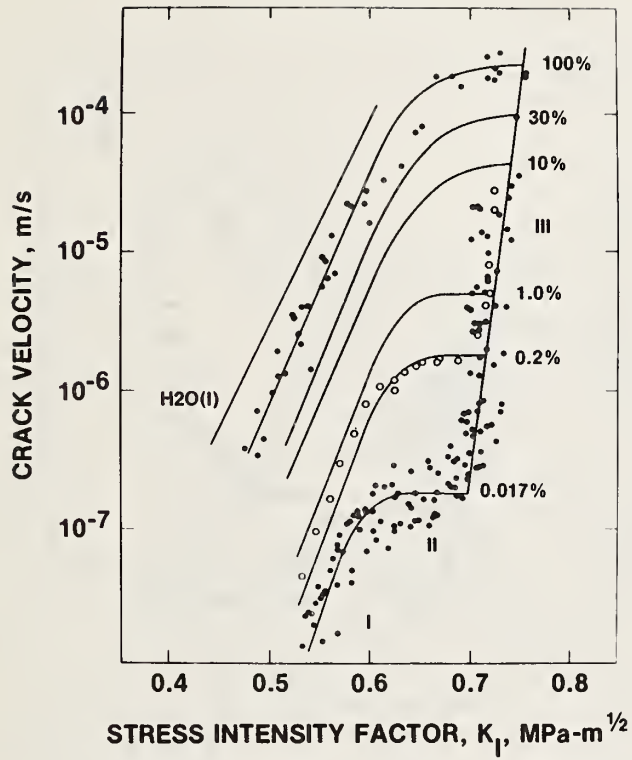


Figure 1. Effect of relative humidity on crack growth in soda-lime-silica glass (ref. 1).

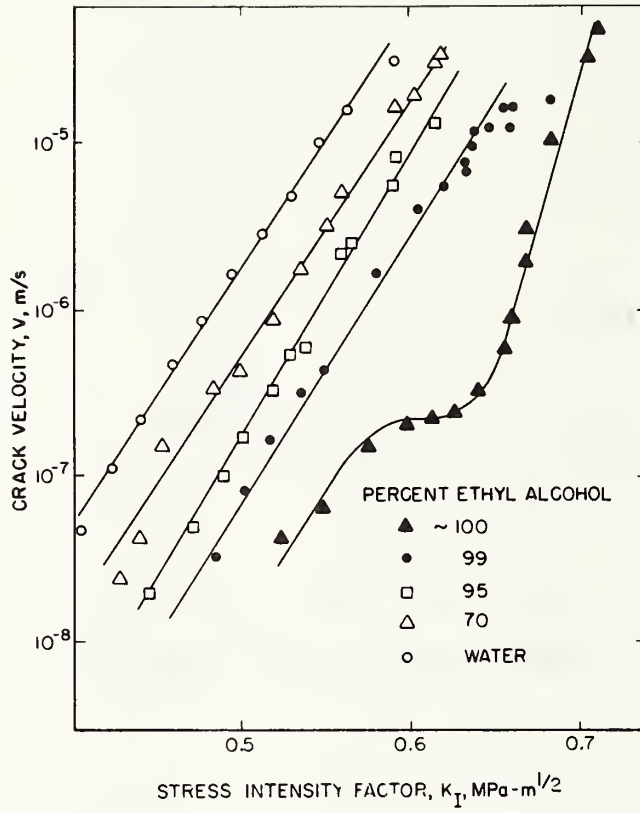


Figure 2. Crack propagation in ethyl alcohol containing water. The concentration of water is expressed in volume percent.

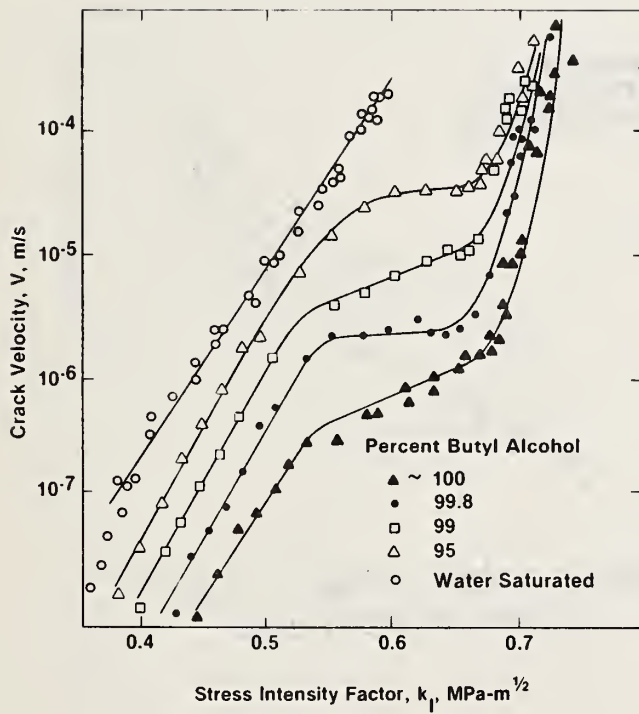


Figure 3. Crack propagation in butyl alcohol containing water. The concentration of water is expressed in volume percent.

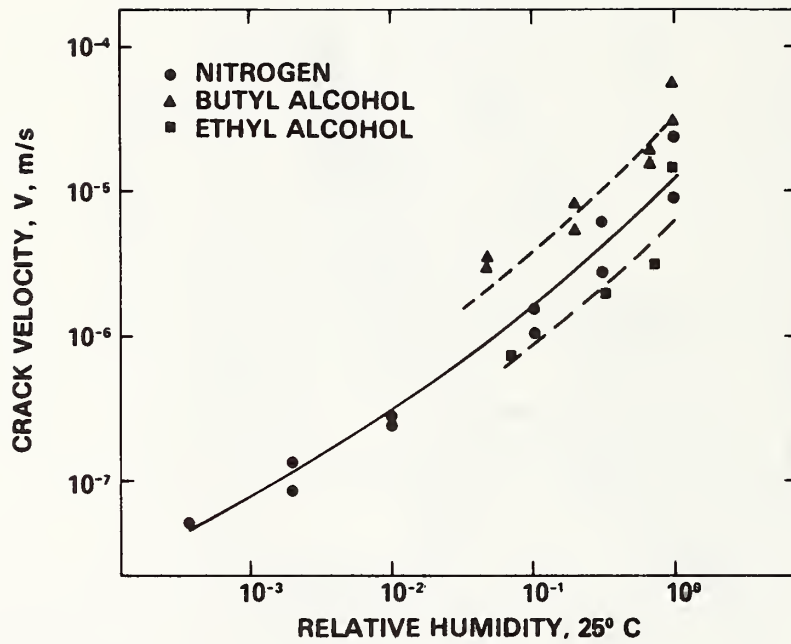


Figure 4. Crack growth rate in region I as a function of relative humidity. Data are taken from figures 2 and 3, at an applied stress intensity factor of $0.563 \text{ MPa}\cdot\text{m}^{1/2}$.

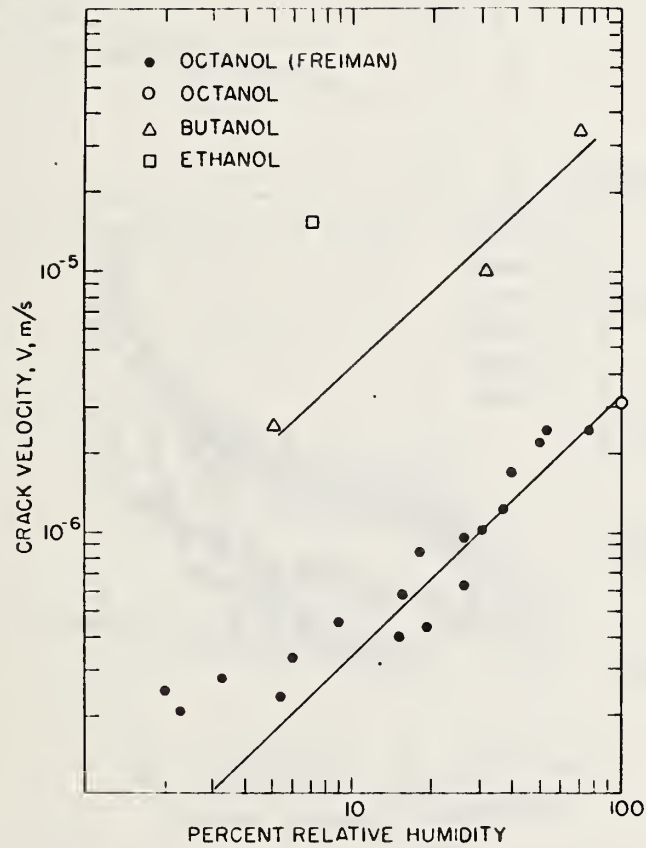


Figure 5. Crack growth rate in region II as a function of relative humidity. The data was taken from figures 2 and 3 using the plateau values of the velocity and relative humidities calculated from the concentration using thermodynamic data reported in references 7 and 8.

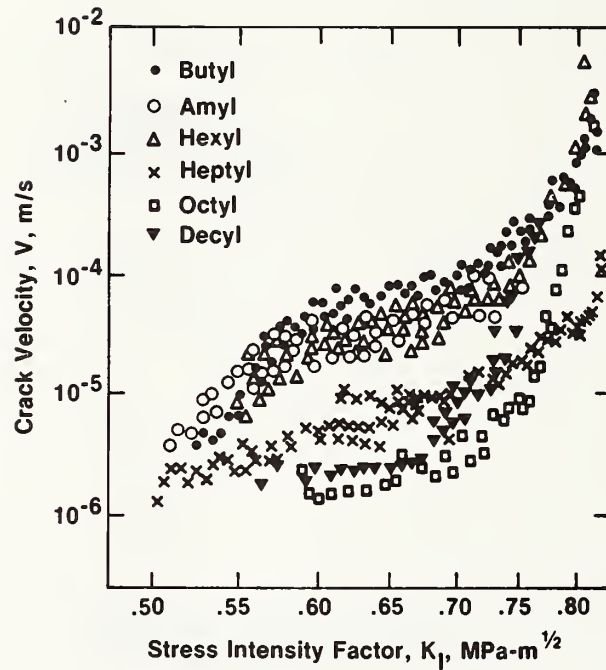


Figure 6. Crack growth data on soda-lime-silica glass collected by the double torsion technique (relaxation method) in alcohols. With the exception of the octyl alcohol, all alcohols were fully saturated. The octyl alcohol was ~50 percent saturated.

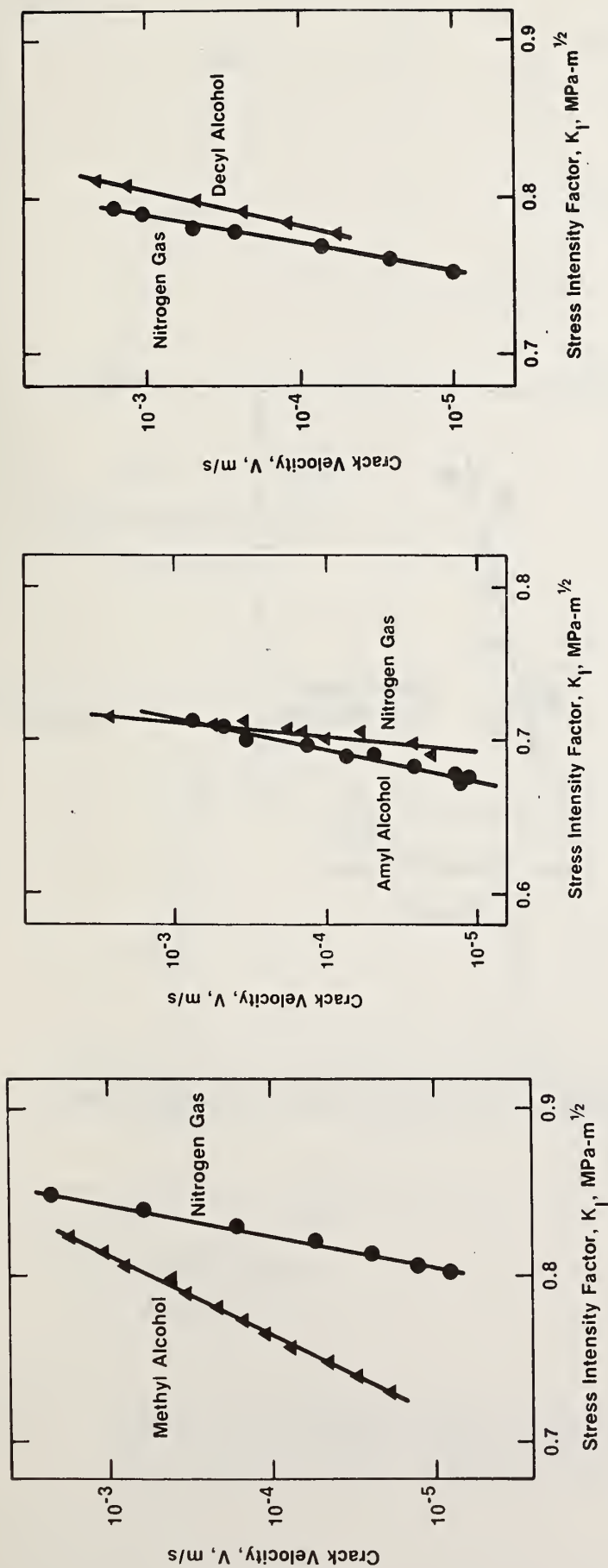


Figure 7. Region III crack growth data collected on soda-lime-silica glass by the double torsion technique (relaxation method) in dry nitrogen gas, and in methyl, amyl and decyl alcohols. Note the shift in the curve to higher values of K_I and the increase in the slope of the crack growth curve as the chain length of the alcohol is increased.

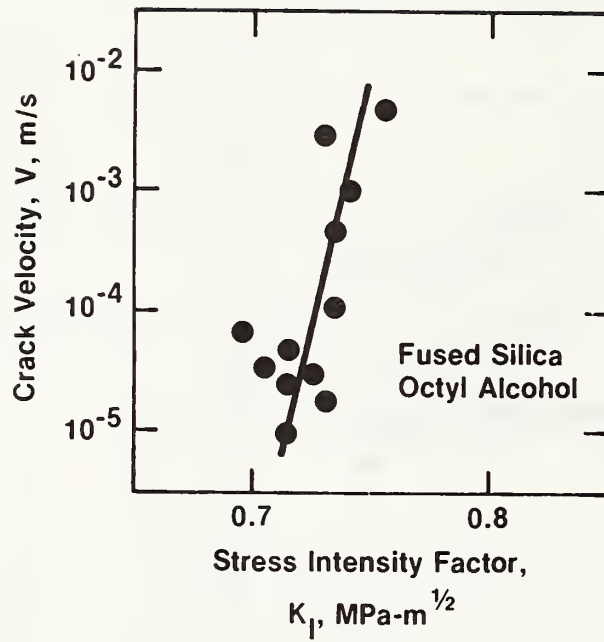


Figure 8. Region III crack growth data collected on silica glass (C7940) by the double cantilever beam technique (constant moment method).

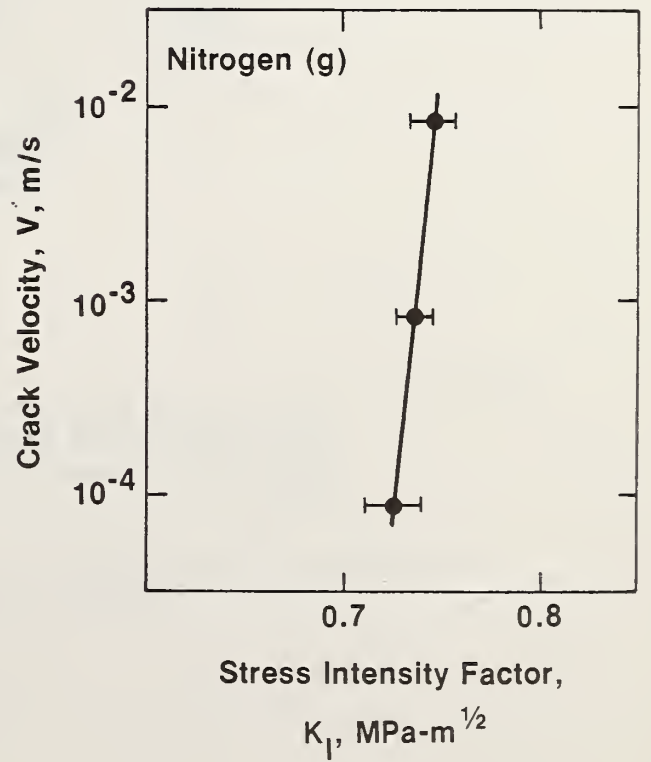
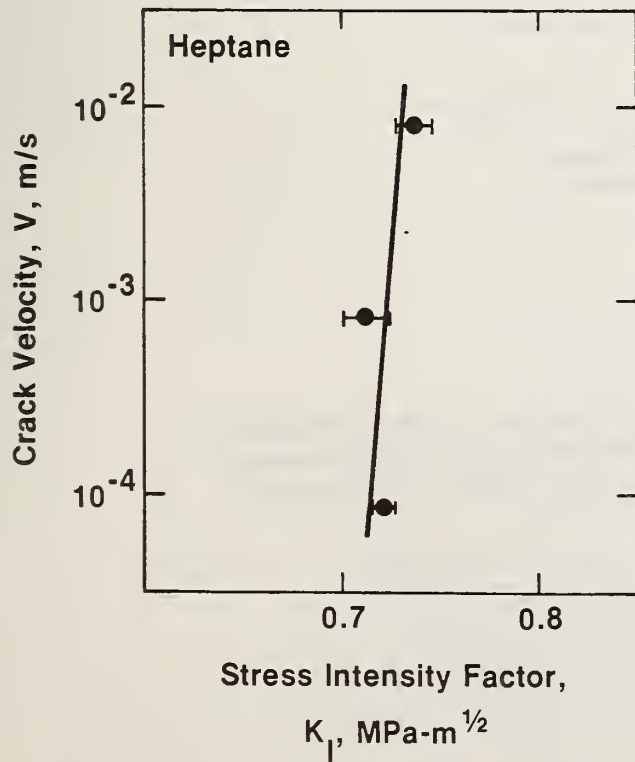
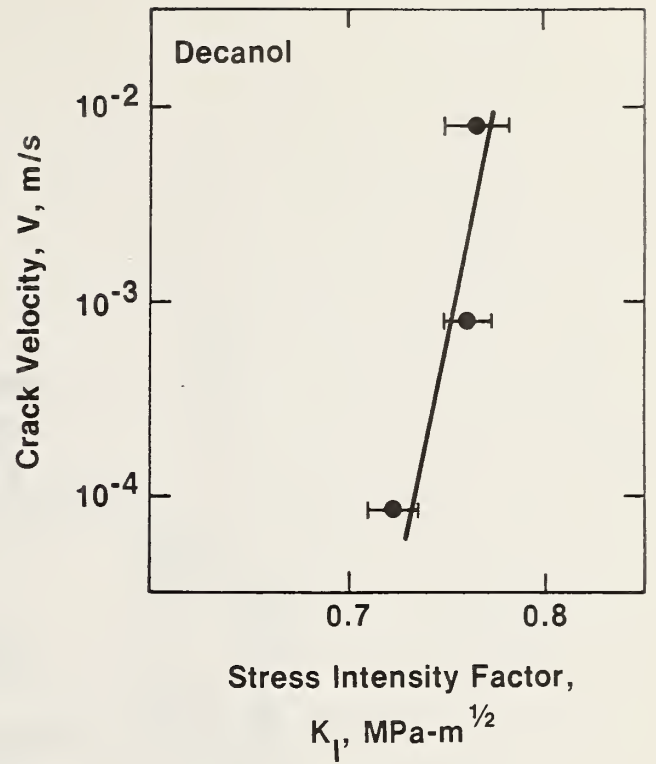
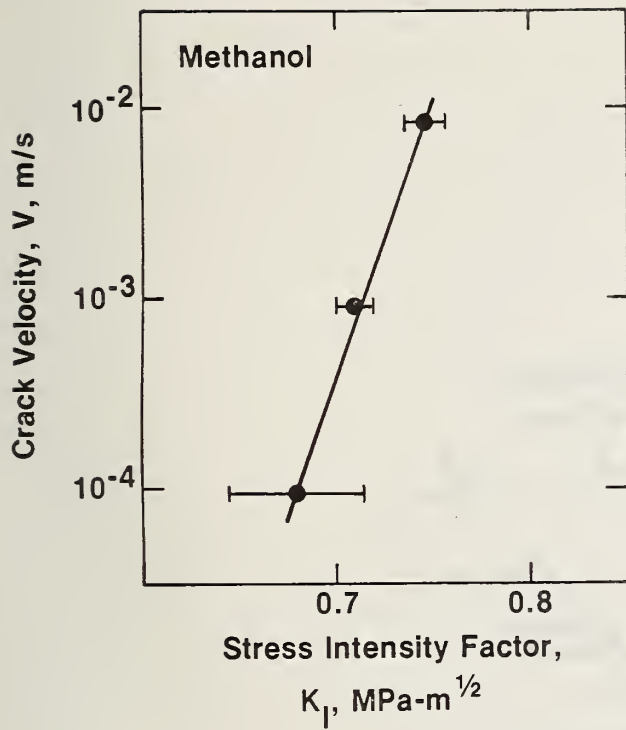


Figure 9. Region III crack growth data collected on soda-lime-silica glass by the double torsion technique (plateau method) in dry nitrogen gas and in methyl alcohol, decyl alcohol and heptane.

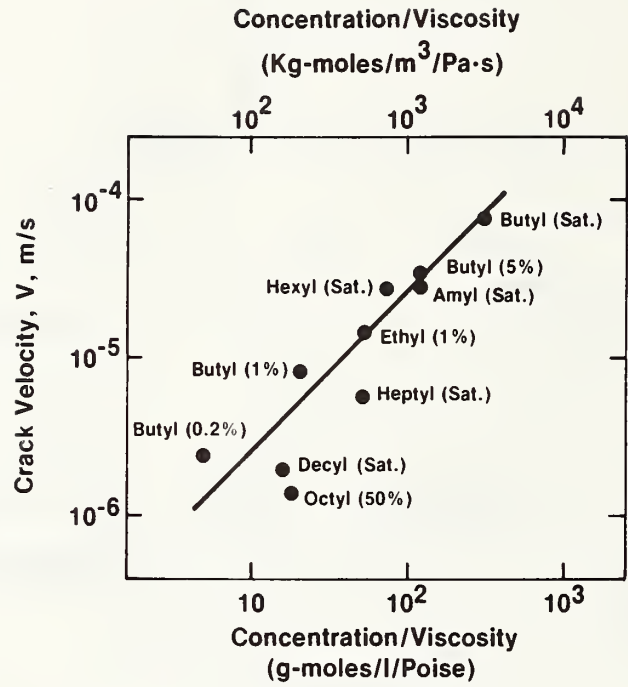


Figure 10. Plot of the crack velocity in region II as a function of the ratio of the molar concentration to the viscosity. Crack growth data on the alcohols taken from figures 2, 3 and 6.

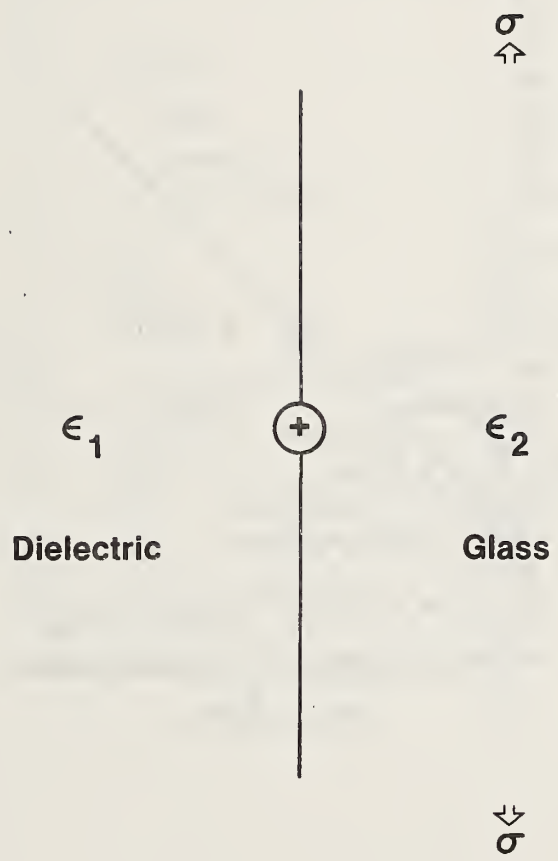


Figure 11. Schematic of model used to determine the electrostatic component of the activation volume.

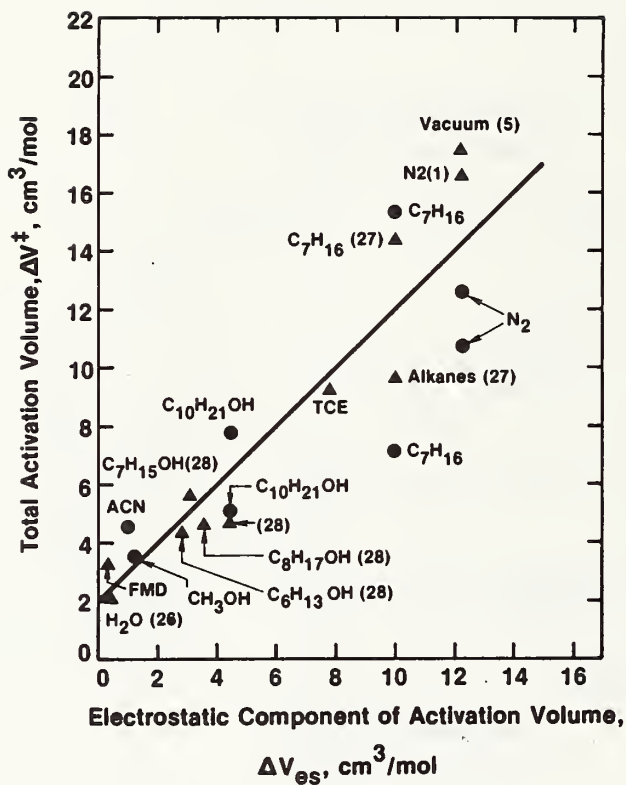


Figure 12. Plot of the total activation volume (eq. 9) as a function of the electrostatic component of the activation volume (eq. 15). The value of $\partial\epsilon_1/\partial P$ ($-9.72 \times 10^{-11} \text{ Pa}^{-1}$) was taken from data by Colwell³⁰ collected on an alkali containing glass made at NBS. Double cantilever beam data are indicated by circles, double torsion data by triangles. Data taken from the literature are identified by reference numbers on the figure. ACN is an abbreviation for acetonitrile; FMD is an abbreviation for formamide; TCE is an abbreviation for trichlorethylene. The other chemical symbols are standard chemical designations.

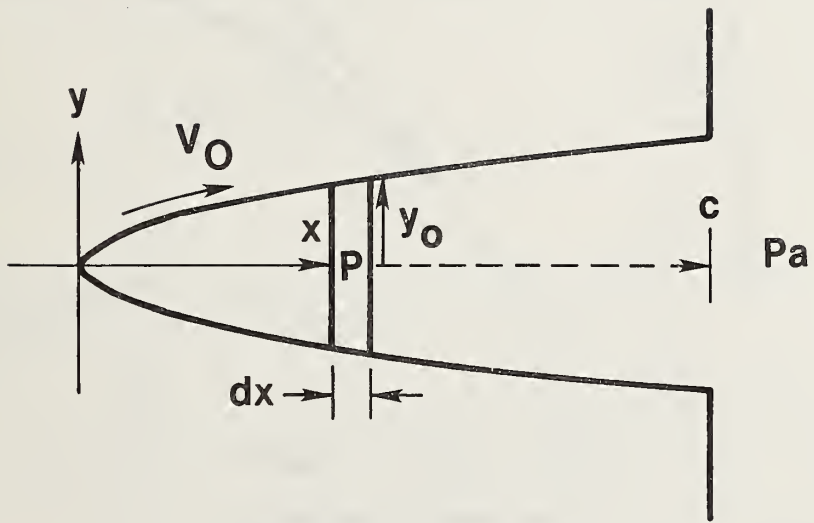


Figure 1A: Schematic diagram of parabolic shaped surface crack.

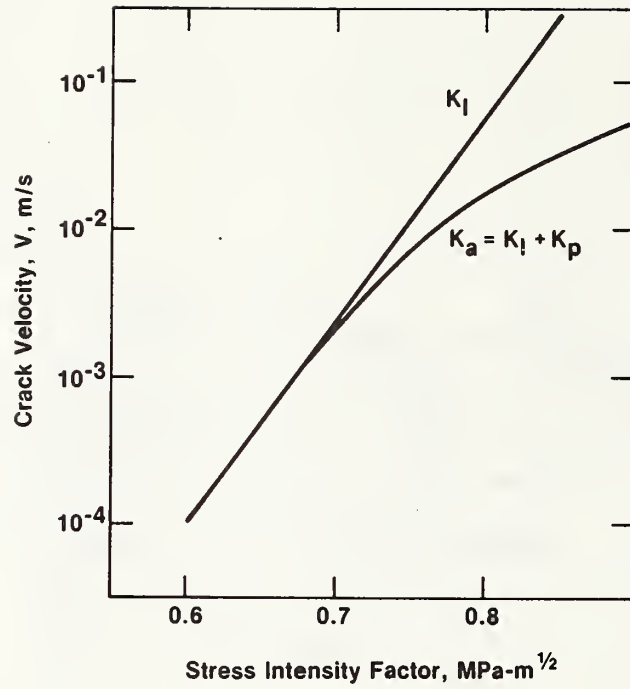


Figure 2A: Calculated effect of fluid viscosity on v - K_I curve: soda-lime-silica glass in water. The K_I portion of the curve is linear extrapolation of data collected at velocities less than 10^{-3} m/s.

U.S. DEPT. OF COMM. BIBLIOGRAPHIC DATA SHEET <i>(See instructions)</i>	1. PUBLICATION OR REPORT NO. NBSIR 82-2524	2. Performing Organ. Report No.	3. Publication Date June 1982
4. TITLE AND SUBTITLE Effects of Water and other Dielectrics on Crack Growth			
5. AUTHOR(S) S. M. Wiederhorn, S. W. Freiman, E. R. Fuller, Jr. and C. J. Simmons			
6. PERFORMING ORGANIZATION <i>(If joint or other than NBS, see instructions)</i> NATIONAL BUREAU OF STANDARDS DEPARTMENT OF COMMERCE WASHINGTON, D.C. 20234		7. Contract/Grant No.	8. Type of Report & Period Covered
9. SPONSORING ORGANIZATION NAME AND COMPLETE ADDRESS <i>(Street, City, State, ZIP)</i>			
10. SUPPLEMENTARY NOTES <input type="checkbox"/> Document describes a computer program; SF-185, FIPS Software Summary, is attached.			
11. ABSTRACT <i>(A 200-word or less factual summary of most significant information. If document includes a significant bibliography or literature survey, mention it here)</i> <p>The effect of water and a variety of organic liquids on the crack growth rate in soda lime silica glass was investigated. When water is present in organic liquids, it is usually the principal agent that promotes subcritical crack growth in glass. In region I, subcritical crack growth is controlled primarily by the chemical potential of the water in the liquid; whereas in region II, crack growth is controlled by the concentration of water and the viscosity of the solution formed by the water and the organic liquid. In region III, where water does not affect crack growth, the slope of the crack growth curves can be correlated with the dielectric constant of the liquid. It is suggested that these latter results can be explained by electrostatic interactions between the environment and charges that form during the rupture of Si-O bonds.</p>			
12. KEY WORDS <i>(Six to twelve entries; alphabetical order; capitalize only proper names; and separate key words by semicolons)</i> Glass; fracture; strength; static fatigue; subcritical crack growth; cracks			
13. AVAILABILITY <input checked="" type="checkbox"/> Unlimited <input type="checkbox"/> For Official Distribution. Do Not Release to NTIS <input type="checkbox"/> Order From Superintendent of Documents, U.S. Government Printing Office, Washington, D.C. 20402. <input checked="" type="checkbox"/> Order From National Technical Information Service (NTIS), Springfield, VA. 22161		14. NO. OF PRINTED PAGES 60	15. Price \$9.00

